Facile fabrication and optical properties of oriented multilayer Al-doped ZnO films

H. HE, H. YU
School of Materials Science and Engineering, Shaanxi University of Science and Technology, China

Al-doped ZnO films are an excellent transparent conducting material. In this paper, we report the orientation and anisotropic arrangement and optical property of the Al-doped ZnO films prepared by sol-gel method and different calcining schedules on the quartz glass substrate. X-ray diffraction, atomic force microscopy, and spectrophotometer were used to characterize the films. Calcining of 700□ for 1h after the preannealing at 400□ for 60min led to a low (002)-preferential orientation and granular grains morphology. Calcining of 700□ for 1h by heating at rate of 200□/min led to a high (002)-preferential orientation and morphology of strip grain parallel to each other and to the surface of substrate. The obvious optical anisotropy of the film was observed. The high (002)-oriented films aligning horizontally the strip grains to the substrate show higher transmittance in range of UV-visible light and greater band gap energy. The mechanism of the formation and optical property of oriented films are discussed.

(Received June 18, 2009; accepted July 20, 2009)

Keywords: ZnO:Al film, Sol-gel method, Orientation, Optical anisotropy, Transmittance, Band gap

1. Introduction

Zinc oxide (ZnO) is a wide band gap II–VI semiconductor (3.34 eV) with very attractive properties, including high transparency in the visible wavelength, a high piezoelectric constant, a large electro-optic coefficient [1] and a large exciton binding energy (□60 meV) at room temperature. Many studies have recently focused on the ZnO films because of their potential application in solar cells, gas sensors, piezoelectric transducers and varistors [2–7]. Some dopants, such as Al, Si, In and Ga, often can improve the electrical and optical properties of ZnO films [8–10]. Al-doped ZnO (AZO) films especially show good electrical and optical properties, and so become an alternative material to tin oxide and indium tin oxide (ITO) that are commonly used as transparent conducting oxides (TCOs). Due to their unique combination of interesting piezoelectric, electric and optical properties, Al-doped ZnO nanomaterials possess great promise for multifunctional applications.

Many factors can affect the properties of aluminum doped ZnO films prepared by sol-gel method. Aluminum content, annealing temperature, component distribution, and crystalline size have significant effect on the optical and electrical properties of the film. Here, we reported investigated effect of annealing schedule on the orientation and optical anisotropy of the Al-doped ZnO films prepared by sol-gel method on the quartz glass substrate.

2. Experimental procedure

$ZnNO_3$ and $Al(NO_3)_3$ dissolved in ethanol at a molar ratio of 99: 1, approximate amount of triethanolamine and glycol ethanol were added to stabilize the solution. Small amount of concentrated hydrochloric acid was added for prevent the formation of hydroxide. The concentration of Zn^{2+} cation in the solution was 0.01M. The film was dip coated on quartz glass substrate with length of 30mm, width of 10mm and thickness of 5mm. After coating, the film was dried at 120 □ for 5-10 min. The five layer films were obtained by repeating the dip coating and the drying. The as-dried films were annealed using the following two schedules. (i) the films were preannealed at 400 □ for 60 min followed by insert the film to a furnace at 600 □ and 700 □ and annealed for 60 min, respectively, (noted as S61 and S71); (ii) the films were rapidly put into a furnace at 600 □ and 700 □ and annealed for 60 min, respectively, (noted as S62 and S72).

The phase of the deposited ZnO: Al thin films were identified at room temperature using X-Ray diffractometer (XRD, $CuK_{\alpha 1}$, λ=0.15406nm, Model No: D/Max-2200PC, Rigaku, Japan). The morphology and texture of the films were analyzed using atomic force microscopy (AFM, Model No: SPI3800N, Japan). The light transparent of the films were determined with UV-vis spectrophotometer (Model No: 752N, China). The luminescence of the ZnO: Al films were measured on the luminescent spectrophotometer (Modal No: LS-55, PE, US).

3. Results and discussion

Fig. 1 and Fig. 2 shows the XRD patterns of the ZnO: Al films. The wurtzite ZnO is an only XRD detectable phase of the films. The orientation degree of the films was calculated with the XRD data analysis and was summarized in Table 1.

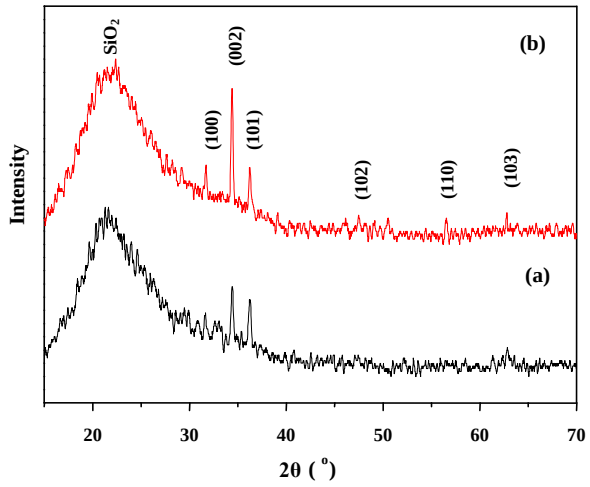

Fig. 1. XRD patterns of the five layers ZnO: Al films preheated at 400 □ and then annealed at (a) 600 □ and (b) 700 □.

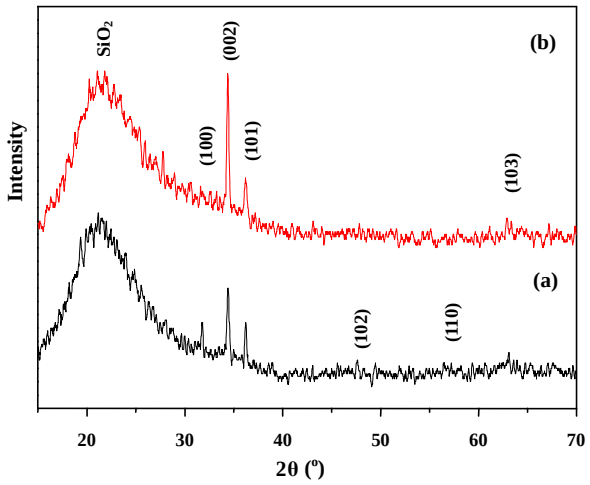

Fig. 2. XRD patterns of the five layers ZnO: Al films direct annealed at (a) 600 □ and (b) 700 □.

In comparison with the standard XRD intensity ratio of $I_{(002)}/I_{(101)}$ =0.44 of the ZnO powder, the films show (002)-preferential orientation to different extent. The (002)-preferential orientation appears very intense when the films were directly annealed without the preannealing and was enhanced with the increase in the annealing temperature. Lattice parameter of the films was calculated by XRD data analysis and is listed in Table 1. The calculated data are slightly larger than that of the pure ZnO powder. This could result from weak crystallinity although less radius of Al^{3+} ion (0.50 Å) compared with the Zn^{2+} ion (0.74 Å). The c/a ratios of the films close to 1.602 of ZnO. The films directly annealed without preannealing all appear greater c./a ratio than the films annealed with the preannealing, which agrees with the variation of the $I_{(002)}/I_{(101)}$. Similarly, some ferroelectric films with c-orientation texture all show great c/a ratio, as reported in literatures [11-13]. The grain size can affects the properties of the film. Calculated from the strongest XRD peaks of the film with Scherrer's formula, Table 1 lists the average particle sizes of all samples. The films directly annealed have relative big size compared with the preanealed films, for which the relative high crystallinity should be responsible.

The Zn–O bond length *L* is calculated by [14,15]

$$L = \sqrt{a^2/3 + \left(1/2 - u\right)^2 c^2} \qquad (1)$$

where the *u* parameter in the wurtzite structure is given by

$$u = a^2/3c^2 + 0.25 \qquad (2)$$

The Zn–O bond lengths calculated are given in Table 1.

Table 1. Lattice parameter, orientation degree and particle size of the ZnO: Al films determined with XRD data analyses.

Heating schedule	Lattice parameter			L (Å)	Orientation degree $I_{(002)}/I_{(101)}$	Particle size (nm)
	a(Å)	c(Å)	c/a			
S61	3.2539	5.2108	1.6014	1.9800	1.21	22.6
S62	3.2548	5.2128	1.6016	1.9806	2.39	38.0
S71	3.2538	5.1988	1.5978	1.9785	2.00	33.7
S72	3.2523	5.2086	1.6015	1.9791	3.40	39.7
ZnO	3.25	5.207	1.602	1.9779	0.44	

Fig. 3 shows AFM micrographs of the ZnO: Al films. The films annealed at 600 □ with and without the preanealing show respectively sphere grains about 100nm and long unregular grains about 600 nm parallel to the substrate surface (Fig. 3(a) and (b)), which are greatly bigger than that of the films annealed at higher temperature of 700 □. This would indicate that the films are amorphous to some extent or crystalline, corresponding to the low crystalline peaks in the XRD patterns. The film annealed at 700 □ after preannealing of 400 □ shows morphology of spherical grains consisting of the big grain of 120 nm and small grain of 15nm (Fig. 3(c)). However, the film directly annealed at 700 □ without preannealing shows morphology of stripy grains with approximate size about 30 nm in width and 160nm in length, which is parallel to each other and lying in growth plane (Fig. 3(d)). The formation of the different morphologies of the films could be attributed to the effects of the annealing schedule and the substrate. The preannealing at 400 □ results in formation of granular nuclei in the films. An epitaxial overgrowth process originating at the nuclei take place in process of the following annealing at 700 □, which lead to the morphology of the spherical crystal grains. In case of no preannealing, the substrate surface at bottom of the film has lower temperature because of the thicker substrate, and so the films can be nucleated originating at the surface of the substrate in process of the rapid heating to 700 □. The hexagonal wurtzite ZnO is of a lattice parameter of a=3.25 Å and c=5.207 Å, so c-axis direction of the film has better lattice matching with the quartz glass closed to quartz crystal (a=0.4913 Å). This promotes the nucleation and the following epitaxial crystal growth of the films along c-axis, and so results in formation of the strip grains running parallel to the substrate surface. The c-axis of the grains may be in long direction of the strip grain, which can be further confirmed by the high c-orientation of the film in the XRD patterns. In some cases, the rapid heating can also results in bulk nucleation throughout the film originating at film surface, the formed nuclei is columnar grains perpendicular to substrate surface, at which the columnar film pendicular to the substrate can be epitaxially formed in process of following annealing. It could be possible that columnar nucleation formed in heating process and the nucleation effect of the substrate comprehensively led to the formation of the strip morphology of the ZnO:Al films, in which the substrate effect could be superior. The thickness of the films is about 270 nm from the AFM analysis.

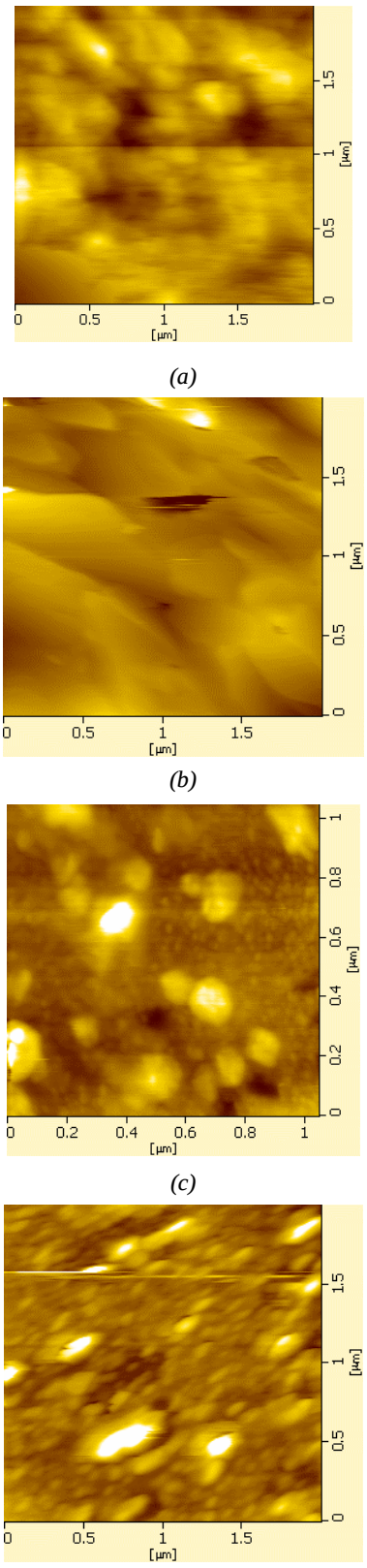

Fig. 3. AFM micrographs of the five layer ZnO: Al films (a) preannealed at 400 □ and annealed at 600 □, (b) direct annealed at 700 □, (c) preannealed at 400 □ and annealed at 700 □, (d) annealed at 700 □.

Fig. 4 shows transmittance spectra of the ZnO: Al films prepared with different annealing schedules. It is clear that the films have high transparency in the UV-visible range, which is obviously larger for the directly annealed films than the preannealed films. In addition, a blue shift of absorption were observed for the directly annealed films compared with the preannealed films. This could originate from optical anisotropy of the ZnO: Al crystal. That is, the films have greater polarized optical transmittance and blue shift of absorption edge in direction parallel to the c-axis compared with that in direction perpendicular to the c-axis, as reported in literatures [16-18]. The polarized optical transmittance and blue shift in direction parallel to the c-axis could increase as increase in the aspect ratio of the grains. Thus, the higher is the difference in aspect ratio of the grains is, the higher is the transmittance difference and blue shift of the film. Furthermore, the films annealed at 700 □ show greater transmittance than the films annealed at 600 □ in either cases of the preannealing and direct annealing. Greater crystallinity could be a main reason. The sharp peaks near 603 nm could correspond to the luminescence emission of the films.

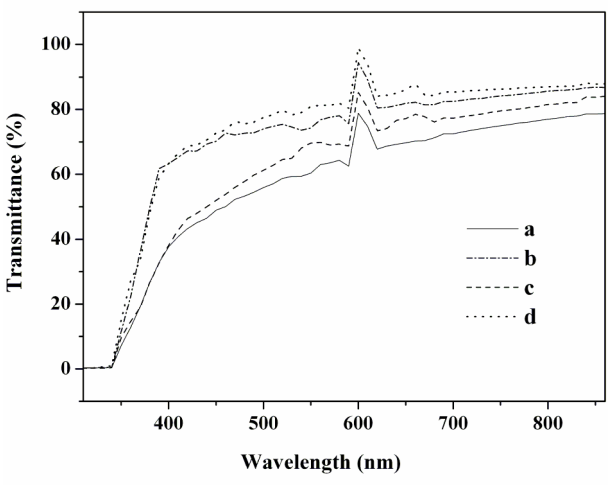

Fig. 4. Transmittance spectra of the ZnO: Al films (a) preannealed at 400 □ and annealed at 600 □, (b) direct annealed at 700 □, (c) preannealed at 400 □ and annealed at 700 □, (d) annealed at 700 □.

Wurtzite structure ZnO has a direct band gap, the optical band gap (E_g) can be calculated with the following relationship [19]:

$$(\alpha h\nu)^2 = C(h\nu - E_g) \quad (3)$$

where $h\nu$ is photon energy and C is a constant between 10^{14} and 10^{16} eV•m^{-2} [15], and α is absorption coefficient, we assume

$$\alpha = \left(1/d\right)\left(\ln 1/T\right) \quad (4)$$

where T is the transmittance and d is the film thickness. Fig. 5 shows the graph of $(\alpha h\nu)^2$ vs. photon energy $h\nu$ for the ZnO: Al thin films prepared with different annealed schedules. The linear dependence of $(\alpha h\nu)^2$ on $h\nu$ at higher photon energies indicates that the ZnO:Al films are essentially direct-transition-type semiconductors. The straight-line portion of the curve, when extrapolated to zero, gives the optical band gap E_g (Table 2). The constant C was calculated with the reciprocal gradient of the linear portion in these curves. The calculated results are listed in Table 2.

Table 2. band gap energy (E_g) and constant C of the ZnO: Al films.

Heating schedule	E_g (eV)	C (10^{15} eV×m^{-2}
S61	3.45	3.97
S62	3.48	4.88
S71	3.46	4.06
S72	3.48	4.94
ZnO	3.34	

From the results of Fig. 5, E_g for the ZnO:Al thin films is 3.45-3.48 eV. These values are all greater than 3.34eV of pure ZnO. This broadening in the band gap is the known Moss–Burstein shift resulted from Al-doping and quantum size effect of the films with nano-particle size. Difference in band gap between the ZnO: Al thin films with different morphologies could be mainly related to the optical anisotropy of the films.

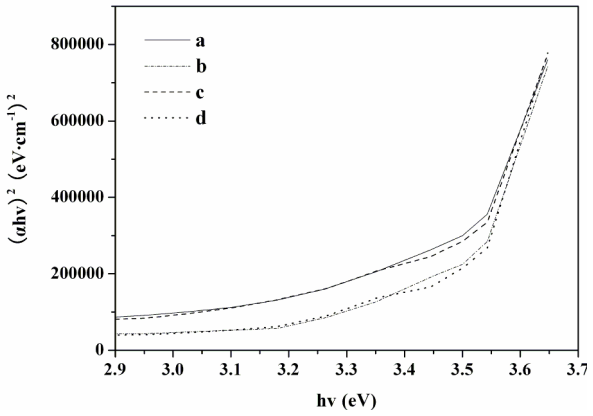

Fig. 5. Plots of $(\alpha h\nu)^2$ vs. hv for ZnO: Al films (a) preannealed at 400 □ and annealed at 600 □, (b) direct annealed at 700 □, (c) preannealed at 400 □ and annealed at 700 □, (d) annealed at 700 □.

Fig. 6 illustrates the photoluminescence spectra of ZnO: Al films annealed at 700 □. It is obvious that the films show blue-green emission.

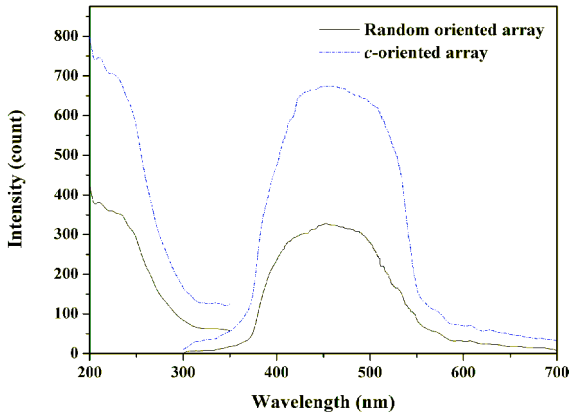

Fig. 6. Luminescence spectra of the ZnO: Al films annealed at 700°C.

The c-oriented film has more intense emission compared to the randomly orientation oriented film. The ZnO material generally exhibits visible emission in green, yellow and orange regions. In general, visible emission is attributed to the native defects in ZnO. The blue-green emission is attributed to the singly ionized oxygen vacancy (*VO*+) and also doubly ionized oxygen vacancy (*VO*++)[20].

4. Conclusions

The ZnO: Al films have been successfully fabricated on the quartz glass substrate with a sol-gel method. The high (002)-preferential oriented films with the morphology of strip grains parallel to each other and to the quartz glass substrate can be achieved by annealing sample after the heating at rapid rate. This film shows higher transmittance in range of UV-visible light and higher band gap energy in comparison with the low (002)-preferential oriented films with a grain morphology fabricated by preannealing at 400□. This is of importance to the optical application of the ZnO: Al film.

References

[1] D. L. Polla, R. S. Muller, R. M. White, IEEE Electron Device Lett. **7**, 254 (1996).
[2] W. J. E. Beek, M. M. Wienk, R. A. J. Janssen, Adv. Funct.Mater. **16**, 1112 (2006).
[3] Z. L. Wang, J. H. Song, Science **312**, 242 (2006).
[4] J. X. Wang, X. W. Sun, Y. Yang, H. Huang, Y. C. Lee, O. K. Tan, L. Vayssieres,, Nanotech. **17**, 4995 (2006).
[5] H. Y. Liu, H. Kong, X. M. Ma, W. Z. Shi, J. Mater. Sci. **42**, 2637 (2007).
[6] V. Gupta, A. Mansingh, J. Appl. Phys. **80**, 1063 (1996).
[7] M. Bertolotti, M. V. Laschena, M. Rossi, A. Ferrari, L. S. Qian, F. Quaranta, A. Valentini, J. Mater. Res. **5**, 1929 (1990).
[8] G. A. Hirata, J. Mekittrik, T. Cheek, J. M. Siqueiros, J. A. Diaz, O. Contreras, O. A. Lopex, Thin Solid Films **288**, 29 (1996).
[9] P. Nunes, B. Fernandes, E. Fortunan, P. Vilarinlo, R. Martins, Thin Solid Films **337**, 176 (1999).
[10] K. T. R. Reddy, R. W. Miles, J. Mater. Sci. Lett. **17**, 279 (1998).
[11] R. W. Schwartz, P. G. Clem, J. A. Voigt, et al, J. Am. Ceram. Soc. **82**(9), 2359 (1999).
[12] S. Hoffmann, U. Hasenkox, R. Waser, J. L. Jia, K. Urban, Mater. Res. Symp. Proc. **474**, 9 (1997).
[13] H. He, J. Huang, L. Cao, Mat. Res. Innov. **12**(2), 66 (2008).
[14] C. S. Barret, T. B. Massalski, Structure of Metals, Pergamon Press, Oxford, 1980.
[15] S. Ilican, Y. Caglar, M. Caglar, J. Optoelectron. Adv. Mater. **10**(10), 2578 (2008).
[16] C. R. Gorla, N. W. Emanetoglu, S. Liang, W. E. Mayo, Y. Lu, J. Appl. Phys. **85**, 2595 (1999).
[17] M. Wraback, H. Shen, S. Liang, C. R. Gorla, Y. Lu, Appl. Phys. Lett. **74**, 507 (1999).
[18] D. M. Schaadt, O. Brandt, S. Ghosh, T. Flissikowski, U. Jahn, H. T. Grahn, Appl. Phys. Lett. **90**, 231117 (2007).
[19] N. Serpone, D. Lawless, R. Khairutdinov, J. Phys. Chem. **99**, 16646 (1995).
[20] V. Rakhesh, M. Junaid Bushiri, V. K. Vaidyan, J. Optoelectron. Adv. Mater. **9**(12), 3740 (2007).

*Corresponding author: hehy@sust.edu.cn